Control of Molecular Energy Redistribution Pathways via Surface Plasmon Gating

Gary P. Wiederrecht,[1] Jeffrey E. Hall,[1] and Alexandre Bouhelier[1,2]

[1]*Center for Nanoscale Materials and Chemistry Division, Argonne National Laboratory, Argonne, Illinois 60439, USA*

[2]*Département Nanosciences, Institut Carnot de Bourgogne CNRS-UMR 5209, Dijon, France*

(Received 25 October 2006; published 21 February 2007)

Strong coupling of molecular electronic states with tunable surface plasmon resonances is used to control electronic energy redistribution pathways in molecules adsorbed on a silver film. Ultrafast excitation of porphyrinic molecular J aggregates into the S_2 state is followed by a second pulse of varying incident wave vector to produce a tunable plasmon in the film. When the plasmon overlaps the S_1 state, energy flows from S_2 to S_1 at high efficiency. If the plasmon hybridizes with the S_2 state, the excitation remains in the S_2 vibrational manifold during quenching to the ground state. These results could have significant impact on the design of active molecular devices.

DOI: 10.1103/PhysRevLett.98.083001 PACS numbers: 33.50.−j, 73.20.Mf, 78.66.−w, 82.53.−k

Molecular energy redistribution pathways following photoexcitation can take many forms, including internal conversion between excited states, intersystem crossing, and dipole-dipole coupling between two electronically polarized entities. These processes are frequently the initial steps that launch innumerable and important biological, chemical, and radiative processes. Well-known examples include isomerization of the retinal rhodopsin for optical signal transduction [1], or light harvesting energy transfer via dipole-dipole coupling in photosynthetic reaction centers [2]. Molecular electronic energy redistribution also impacts important high technology issues, such as excited state deactivation responsible for reduced energy conversion efficiencies in solar cells [3], isomerization for molecular electronics and molecular optics applications [4], and the efficiencies of organic light emitting diodes [5]. In many cases, energy redistribution consists of competing processes that fundamentally limit the efficiency of a desired pathway following photoexcitation, such as charge separation, bond breakage, or luminescence. Therefore, the control or selection of a particular energy redistribution channel has been widely pursued experimentally and theoretically [6,7]. We are reporting in this Letter a new means to control ultrafast molecular electronic energy redistribution pathways in molecules on a metal surface through the use of tunable surface plasmon polaritons (SPPs).

The photophysical response of molecules is known to be dramatically altered when placed on a metal surface [8]. This is most commonly due to an increase in radiationless energy redistribution between the excited molecule and the electronic polarizations of the metal [9,10]. It is also established that strong electromagnetic field enhancements can be produced near the surface of a metal [11–13]. This study shows that a strong electronic coupling between molecules and SPPs can be used to direct intramolecular energy flow in a two-pulse transient absorption experiment. Specifically, when the S_2 state of a molecular aggregate exciton is optically excited, the ultrafast energy redistribution can be chosen with high specificity to be either an internal conversion pathway through a lower S_1 excited state or to undergo vibrational relaxation within the S_2 state. This is found to occur when the energy of a SPP, excited by the white light continuum probe, is selected to overlap the molecular excited state through which energy redistribution is desired.

For the molecular system, the J-aggregate meso-tetra(4-sulfonatophenyl) porphyrin ($TSPP^{2-}$) with two energetically different excitons as shown in Fig. 1(a) was chosen. J aggregates are known for forming Frenkel excitons that produce narrowed and redshifted excitonic absorption bands relative to the monomer [14,15]. Molecular J aggregates can interact strongly with SPPs [16,17] due to their very large extinction ($>10^5$ M^{-1} cm^{-1}) and oscillator strength, and are therefore ideal for these studies. Additionally, they can be easily engineered on metal surfaces to create exciton-plasmon hybrid materials [18,19]. These hybrid structures permit a selected molecular exciton and SPP to be excited simultaneously and coherently. In the spectral regions of plasmon excitation, enhancement of the electromagnetic near field produces an anomalously large extinction of the overlapping molecular excited state. At the same time, the excitons, derived from intramolecular excited states, serve to provide an amplified signal of intramolecular processes.

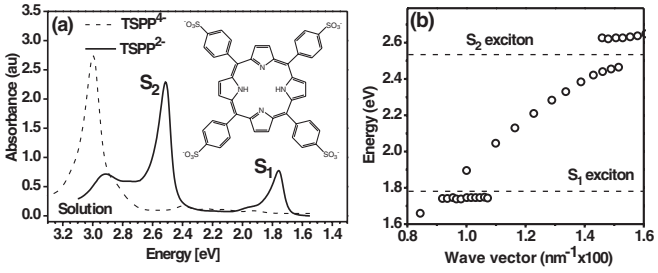

FIG. 1. (a) The ground state absorption spectra for solutions of the monomer ($TSPP^{4-}$) and the J aggregate ($TSPP^{2-}$). The molecular structure of the $TSPP^{4-}$ monomer is shown in the inset. (b) The plasmon-exciton hybrid dispersion curve for the $TSPP^{2-}$ J aggregate on a Ag film.

The hybrid structures were engineered via layer-by-layer (LbL) electrostatic deposition [18–20]. The LbL deposition consisted of first depositing cystamine ($C_4S_2N_2H_{12}$) on a 50 nm thick Ag layer. The acidic $TSPP^{2-}$ solution protonates the amine group to produce a positively charged monolayer that attracts the charged $TSPP^{2-}$ molecules. This is followed by the deposition of poly(diallyldimethylammonium chloride) polymer which creates a positively charged layer on top of the $TSPP^{2-}$ layer. The process was repeated to produce four monolayers of aggregates. To facilitate the excitation of SPPs overlapping a particular exciton band, the plasmon dispersion of the hybrid structure was first determined [21]. A conventional attenuated total internal reflection (ATR) geometry was used to map the dispersive response [22,23], with the results shown in Fig. 1(b) for p-polarized excitation. The figure demonstrates the coupling interaction between the SPP and the excitons as measured by the deformation of the dispersion and can be qualitatively understood as follows. The SPP creates a coherent polarization that can interact strongly with the resonant transitions of the $TSPP^{2-}$. If the interaction is strong enough, the coupling between the SPP and the excitonic state leads to an anticrossing of the dispersion with the appearance of a Rabi splitting [22,24]. The two modes are in a strong coupling regime, otherwise known as hybridization [25]. This situation can be seen in Fig. 1(b) for the S_2 exciton. However, the broader linewidth 1.76 eV S_1 exciton state [Fig. 1(a)] and the SPP are in a weaker coupling regime due to the lower oscillator strength and faster electronic dephasing of the S_1 exciton. No discernible surface plasmon mode splitting is observed at this energy. The isotropic orientation of the transition moment of the aggregates on the surface ensures that they can be efficiently excited with all polarization orientations. However, for a p-polarized excitation, the interaction with the SPP will preferentially select the aggregates' moments aligned perpendicularly to the interface [22]. We note, however, that for an s-polarized illumination SPPs are not excited and the dispersion relations of the two exciton states do not show any dependence on wave vectors.

The exciton dynamics were characterized by ultrafast transient absorption spectroscopy via the two pump-probe geometries depicted in Figs. 2(a) and 2(b). The experiments were performed with an amplified Ti:sapphire laser that outputs 130 fs pulses at 1 kHz and is equipped with an optical parametric amplifier (OPA) described previously [26]. The OPA output is the source of the pump laser pulse, which for these experiments is set at energies to overlap either S_2 or S_1. The probe pulse is a coherent white light continuum that is variably delayed relative to the pump pulse via a mechanical delay line [26]. The broadband probe enables transient spectra (by maintaining constant probe delay and scanning a monochromator) or kinetics (by selecting a probe wavelength with a monochromator and scanning the delay line) to be obtained over the visible and near-infrared energies. This technique is widely used

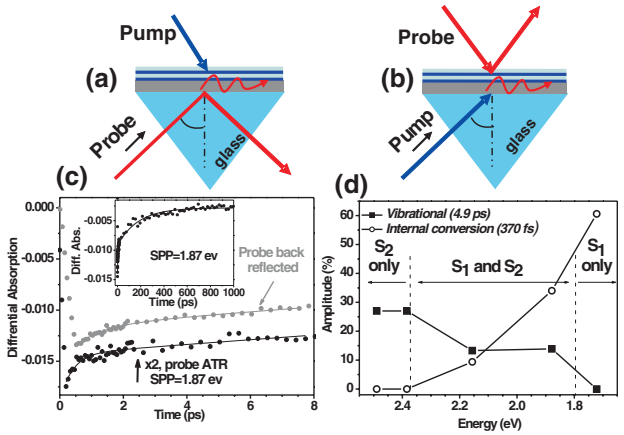

FIG. 2 (color online). (a) The pump-probe ATR geometry used for a selective SPP excitation via the probe pulse. (b) Control geometry which does not allow for the probe to directly excite SPPs (c) S_2 transient kinetics obtained for a probe-induced plasmon energy at 1.87 ev for the ATR geometry (black circles) and for the control geometry (gray circles) with a vertical offset for clarity. The solid curves are multiexponential fits with characteristic decay times of 370 fs, 4.9 ps, 150 ps, and 1.7 ns, and amplitudes as outlined in the text. The data for the control geometry do not have a sub-ps decay for any angle of incidence. The inset shows the full, long time decay of the S_2 kinetics. (d) The amplitudes as a percentage of total ΔA of the 370 fs and 4.9 ps components as a function of the SPP energy excited by the probe pulse.

in many disciplines for monitoring kinetic and mechanistic aspects of photochemical and photophysical events [27].

Only for the ATR geometry [Fig. 2(a)] is a spectral portion of the white light probe coupled to a plasmon of varying energy as determined by the dispersion shown in Fig. 1(b). An example of the kinetics for this system is shown in Fig. 2(c). A pump energy at 2.5 eV excites the molecular aggregate into the S_2 exciton state which is known to be a strongly allowed transition [28]. For the white light probe, an incident wave vector is selected to excite a plasmon at 1.87 eV centered between the S_1 and S_2 resonance. The transient absorption trace reveals two kinetic responses that occur on a sub-10 ps time scale. The first has a response time of less than 600 fs, with an average for all scans of 370 fs, while the second has an average time constant of 4.9 ps. For the purpose of assigning these decay components, the competitive pathways for energy redistribution following photoexcitation of the S_2 exciton were considered. One pathway is internal conversion (IC) into the S_1 state [29]. The time constant for internal conversion in $TSPP^{2-}$ J aggregates was previously determined to be $\sim$300 fs in solution [29]. This value is consistent with the 370 fs component measured in our study and is therefore attributed to IC. To further support this assignment, the pump was tuned to optically excite only the S_1 exciton in the ATR probe geometry of Fig. 2(a). The transient signal probed at S_2 shows a bleach due to the removal of $TSPP^{2-}$ from the ground state following photoexcitation (data not

shown). Importantly, however, no sub-ps kinetics are observed at any incident angle when S_1 is excited, supporting the assignment of this component to IC from S_2 to S_1. Following the internal conversion, radiative decay and dipole-dipole coupling between S_1 and the metal relax the excitation to the ground state on a 50 ps time scale. A second energy redistribution channel considered is vibrational relaxation in the S_2 electronic manifold followed by direct coupling to the metal film polarizations. Past studies of $TSPP^{2-}$ in solution showed that vibrational relaxation within the S_2 electronic manifold occur on a 4–10 ps time scale [29] and is consistent with the 4.9 ps component measured in the present hybrid structure. Finally, a third decay mechanism is trapping of the S_2 exciton at monomer defect sites [18], followed by monomeric excited state return to the ground state. We observe a significant long time decay component of approximately 1.7 ns [inset in Fig. 2(c)] which is slightly shorter than past studies of $TSPP^{2-}$ in solution [29]. However, the shorter monomer lifetime on the metal surface is consistent with a quenching to the ground state.

The 370 fs and 4.9 ps components have opposing amplitude trends vs the plasmon energy excited by the probe beam. As shown in Fig. 2(d), the 370 fs component (IC) dominates the kinetics on the sub-10 ps time scale when the probe is chosen to excite an SPP near the S_1 exciton. The amplitude of the IC component decreases monotonically as the probe-induced SPP is moved from S_1 to the S_2 energy, and is entirely eliminated when the SPP nears the S_2 resonance. On the other hand, the vibrational component (4.9 ps) is the sole sub-10 ps response when the SPP hybridizes with the S_2 exciton. It decreases monotonically in amplitude as the plasmon excited by the probe is moved towards the S_1 state. When the plasmon overlaps the S_1 state, this slower component is absent.

The pump-probe geometry of Fig. 2(b) was used as a control experiment, whereby the probe, reflected off of the top face of the hybrid structure, precluded the possibility of simultaneously exciting an SPP. This geometry only produces the slower component, never the sub-ps component, at all angles of incidence probed [gray circles in Fig. 2(c)]. A second control experiment consisted of establishing the yield of IC between the two excited states without the presence of any SPPs. Continuous wave emission spectra were taken of the $TSPP^{2-}$ aggregates in solution and in a LbL deposition on a glass substrate (data not shown). When excited at the S_2 exciton energy, the solution shows strong emission from the S_1 state at 1.74 eV, but the LbL sample shows no emission. This is consistent with prior studies of similar porphyrinic J aggregates where emission from the S_1 state was considerably weakened in organized assemblies [18,30]. Only when the LbL sample is excited at the S_1 absorption band (exciting at the blue absorption edge at 1.78 eV) is emission from S_1 observed. Therefore, without the presence of an additional gating mechanism, significant population of the S_1 state via IC is drastically reduced in the LbL samples following photoexcitation of S_2.

In the transient spectra for the hybrid films shown in Fig. 3, the only spectrum showing a large spectral response from the S_1 exciton occurs when the probe-induced SPP overlaps the S_1 energy [Fig. 3(b)]. No significant population of the S_1 exciton is ever observed for other SPP energies in our LbL samples [Figs. 3(c) and 3(d)]. This result can be compared to the transient spectrum of Fig. 3(a) which clearly shows that the IC process in solution is active due to the presence of an S_1 differential absorption signal following excitation of S_2. Therefore, we conclude that internal conversion from the S_2 to S_1 exciton state is triggered only when the probe coherently excites an SPP near the S_1 state and dominates initial energy redistribution within the $TSPP^{2-}$ molecular aggregate. To further confirm the gating role of the SPP, transient spectroscopy was performed for different probe powers (one in which the energy of absorbed pump light and incident probe light are equal over similar bandwidths, and one in which the probe light was reduced by 70%) overlapping the S_1 state. As shown by the gray curve in Fig. 3(b), only the S_2 signal is observed at the lower probe power, which demonstrates that the SPP plays an active role in moving population from S_2 to S_1. If the plasmon has a passive role, the same spectra (e.g., the comparative amplitudes of each feature should not change) and kinetics should be observed regardless of probe power.

The opposite dependence vs SPP energy of the slower, sub-10 ps component produces additional evidence for this conclusion [Fig. 2(d)]. In the regime where the SPP hybridizes with the S_2 exciton, the slower component at 4.9 ps dominates the initial ultrafast kinetics. Based on the lack of

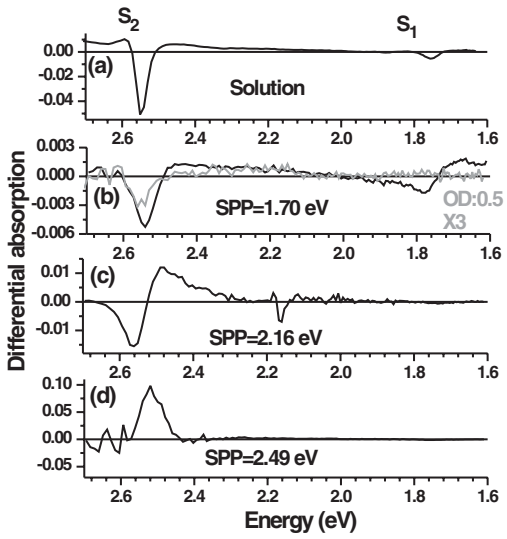

FIG. 3. Transient absorption spectrum of $TSPP^{2-}$ J aggregates at 1.5 ps delay for an excitation at 2.50 ev. (a) Spectrum in solution. (b)–(d) Spectra of the hybrid structure in the ATR pump-probe geometry for three SPP energies excited by the probe.

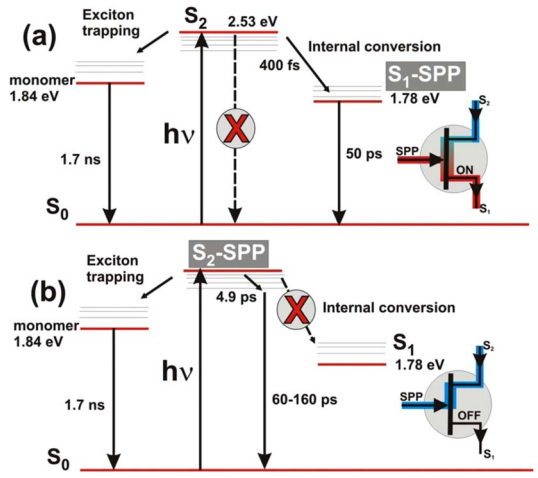

FIG. 4 (color online). Relaxation pathways when the SPP overlaps (a) the S_1 exciton or (b) the S_2 exciton. The process is analogous to an ultrafast all-optical transistor controlling the energy flow from S_2 to S_1 via SPP gating. The transistor is in its ON state for case (a) and OFF state for case (b).

transient spectral features at the S_1 exciton energy shown in Figs. 3(c) and 3(d), population of the S_1 state is minimal for these angles of incidence. We therefore conclude that IC from S_2 to the S_1 state does not play a significant role in energy redistribution when the SPP nears the S_2 resonance. What likely occurs is therefore vibrational relaxation through the S_2 manifold.

Figure 4 summarizes the kinetics of the molecular redistribution processes of the $TSPP^{2-}$ J aggregate on a silver surface. The redistribution process is analogous to an ultrafast molecular optical transistor where the SPP is the gating signal, the S_1 state corresponds to the drain and the S_2 state to the source. When the SPP excited by the probe overlaps the S_1 state, the kinetic processes of Fig. 4(a) apply, with the internal conversion pathway opened and its yield controlled by the intensity of the underlying SPP gate. The S_2 vibrational manifold relaxation remains closed. When the S_2 state is excited and hybridizes with an SPP, the internal conversion pathway to S_1 is closed and the vibrational relaxation within the S_2 manifold is opened. This is followed by quenching of the exciton to the ground state S_0 [Fig. 4(b)].

We propose that this gated mechanism originates from the characteristics of the dispersion curve of Fig. 1(b). When the photoexcited S_2 state and the SPP are in the strong coupling regime, the energy is delocalized only over the two excitations (S_2 and the plasmon), preventing IC to S_1. On the other hand, when the SPP overlaps S_1, the SPP introduces an anomalously large extinction of the overlapping excited S_1 state, triggering and controlling internal conversion from S_2 to S_1.

This work demonstrates a new means to control excited state molecular energy redistribution pathways via a plasmon gating mechanism. These results could have a significant impact on the ability to control the outcome of electronic redistribution processes, thereby influencing the efficiency of photophysical and photochemical processes. This could impact the design of active photonic devices, e.g., an ultrafast molecular transistor with a plasmonic gate, where applications depend on the yield of a desired excited state following photoexcitation.

This work was supported by the U.S. Department of Energy, Office of Science, Office of Basic Energy Sciences, under Contract No. DE-AC02-06CH11357. A. B. gratefully acknowledges the support of the Regional Council of Burgundy.

[1] A. Colonna, G. I. Groma, and M. H. Vos, Chem. Phys. Lett. **415**, 69 (2005).
[2] R. J. Cogdell *et al.*, Photosyn. Res. **81**, 207 (2004).
[3] D. Wrobel, J. Lukasiewicz, and A. Boguta, J. Phys. IV (France) **109**, 111 (2003).
[4] N. Hampp, Chem. Rev. **100**, 1755 (2000).
[5] B. W. D'Andrade and S. R. Forrest, Adv. Mater. **16**, 1585 (2004).
[6] M. Shapiro and P. Brumer, *Principles of Quantum Control of Molecular Processes* (Wiley, New York, 2003).
[7] S. A. Rice and M. Zhao, *Optical Control of Molecular Dynamics* (Wiley, New York, 2000).
[8] P. Anger, P. Bharadwaj, and L. Novotny, Phys. Rev. Lett. **96**, 113002 (2006).
[9] K. H. Drexhage, in *Progress in Optics XII*, edited by E. Wolf (North-Holland, Amsterdam, 1974), p. 163.
[10] H. Kuhn, J. Chem. Phys. **53**, 101 (1970).
[11] D. P. Fromm *et al.*, J. Chem. Phys. **124**, 061101 (2006).
[12] P. Muehlschlegel *et al.*, Science **308**, 1607 (2005).
[13] L. J. Sherry *et al.*, Nano Lett. **6**, 2060 (2006).
[14] E. E. Jelley, Nature (London) **138**, 1009 (1936).
[15] G. Scheibe, Angew. Chem. **49**, 563 (1936).
[16] J. Dintinger, S. Klein, and T. W. Ebbesen, Adv. Mater. **18**, 1267 (2006).
[17] W. L. Barnes, A. Dereux, and T. W. Ebbesen, Nature (London) **424**, 824 (2003).
[18] P. G. V. Patten, A. P. Shreve, and R. J. Donohoe, J. Phys. Chem. B **104**, 5986 (2000).
[19] P. T. Hammond, Adv. Mater. **16**, 1271 (2004).
[20] H. Fukumoto and Y. Yonezawa, Thin Solid Films **327–329**, 748 (1998).
[21] A. Bouhelier and G. P. Wiederrecht, Phys. Rev. B **71**, 195406 (2005).
[22] I. Pockrand, A. Brillante, and D. Mobius, J. Chem. Phys. **77**, 6289 (1982).
[23] V. M. Agranovitch and A. G. Malshukov, Opt. Commun. **11**, 169 (1974).
[24] J. Bellessa *et al.*, Phys. Rev. Lett. **93**, 036404 (2004).
[25] D. G. Lidzey *et al.*, Nature (London) **395**, 53 (1998).
[26] S. R. Greenfield and M. R. Wasielewski, Appl. Opt. **34**, 2688 (1995).
[27] W. Castleman, Jr., *Femtochemistry VII: Fundamental Ultrafast Processes in Chemistry, Physics, and Biology* (Elsevier, Amsterdam, 2006).
[28] Y. Kurabayashi *et al.*, J. Phys. Chem. **88**, 1308 (1984).
[29] H. Kano and T. Kobayashi, J. Chem. Phys. **116**, 184 (2002).
[30] Z. Zhang *et al.*, Langmuir **13**, 5726 (1997).